Observation of Long Equatorial Waves in the Pacific Ocean by Seasat Altimetry

JEAN-PIERRE MALARDÉ*,†, PIERRE DE MEY**, CLAIRE PÉRIGAUD* AND JEAN-FRANCOIS MINSTER**

*Laboratoire de Physique et Chimie de l'Hydrosphère (LA196), 4 Place Jussieu, Paris, France; **Groupe de Recherches de Géodésie Spatiale (UM39) 18 Avenue Edouard Belin, Toulouse, France

(Manuscript received 1 August 1985, in final form 29 April 1987)

ABSTRACT

Synoptic maps of the mesoscale dynamic topography in a band between 7.5°N and 7.5°S in the Pacific Ocean are drawn from Seasat altimeter data. They show a set of eddies 600 km in diameter and 15–20 cm in amplitude moving westward with a velocity of about 40 km day^{-1} along 4.5°N. Their occurrence is consistent with the surface temperature front undulations observed by Legeckis. South of the equator the signal is less coherent, but a significant degree of symmetry with the north is evidenced. The dynamics of the wave system might also present some degree of nonlinearity, as some water seems to be carried along with the wave.

1. Introduction

Trapped long equatorial waves with periods of 20 to 80 days and with a westward phase velocity of 30 to 50 km day^{-1} have been observed repeatedly from satellite sea-surface temperature (SST) maps by Legeckis, in both the Atlantic and the Pacific oceans (Legeckis, 1977; Legeckis et al., 1983; also Weissberg et al., 1979; Weissberg and Horigan, 1981). Theoretical studies indicate that they could result from barotropic instabilities in the strong shear region between the South Equatorial Current (SEC) and the North Equatorial Counter Current (NECC), near 4°N latitude (Philander, 1978; Cox, 1980).

Sea-level monitoring reveals that a clear dynamic topography effect can be associated with these waves (Wyrtki, 1978; Philander et al., 1985; Miller et al., 1985). In particular, Miller et al. analyzed the data from a meridional section of inverted echosounders between the equator and 9°N along 110°W. They observed oscillations of amplitude 10 dyn cm with a predominantly monthly period, correlated with the SST wave patterns. They interpret their results as an oscillating pressure field superimposed on the mean field associated with the SEC/NECC topography ridge. This is also consistent with the trajectories of surface drifters which evidenced the presence of anticyclonic eddies just north of the cusped waves of the thermal front (Hansen and Paul, 1984). This is schematized in Fig. 1.

The present work analyzes the mesoscale dynamic topography in the equatorial Pacific Ocean, as inferred from Seasat altimeter data. The global Seasat mesoscale variability maps (Cheney et al., 1983) reveal a belt of stronger signal around 4°N. It is thus tempting to examine whether this signal is contributed by the long equatorial waves. The unique coverage of the satellite tracks will allow a quasi-synoptic description of the equatorial band. In addition, we expect to gain unprecedented information about the areas south of the equator and west of 160°N, where few classical data are available.

2. Data analysis

If one assumes that eddies are moving westward with a 40 km day^{-1} phase velocity and that they are separated by about 1000 km, any track of the Seasat repeat orbit should have sampled the passage of about one full eddy during its 24 day lifetime. As a consequence, along any given track the signal relative to the average would vary between a maximum of the order of 5–10 cm when the eddy is centered on the track and a corresponding negative minimum between two eddies (see the discussion by Colton and Chase, 1983). In addition, since an ascending and a descending track are separated by about 500 km near 5°N, any eddy should be sampled by one or two tracks at any given time.

We considered the Seasat altimeter data over a band of 24° latitude centered over the equator. They consist of 33 repetitive tracks of eight passes, each from 15 September to 10 October 1978. Ionospheric, tropospheric (using the FNOC water vapor contents, Tapley et al., 1982) sea-state corrections (7% of significant wave height) were applied. The tidal signal from Schwiderski's model (1980) was removed. Spurious data were scanned following a number of criteria described in Périgaud et al. (1986). This eliminated about 3% of the data points. Remaining aberrant data were further discarded with a test limitating the maximum spatial discontinuity between four consecutive points to 60 cm.

† Permanent address: GDTA/ALGOS, 18 Avenue Edouard Belin, 31055 Toulouse Cedex, France.

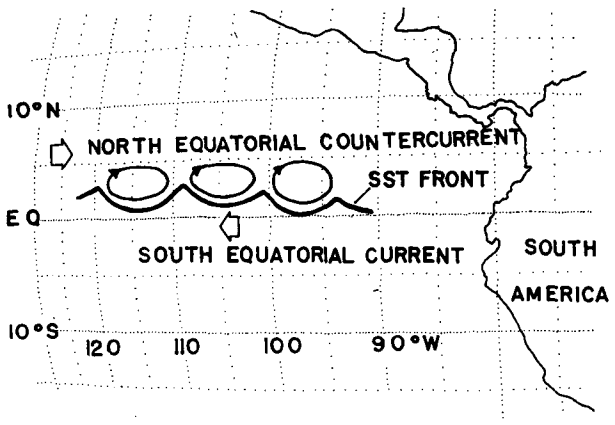

FIG. 1. Schematic representation of the wavelike sea-surface temperature front in the eastern tropical Pacific Ocean. The anticyclonic eddy patterns are inferred from buoy trajectories. After Legeckis et al. (1983).

This further eliminated 1.3% of the data. This created a number of small gaps along the tracks: they were filled in by projecting onto the tracks the average of the previous and following passes along the same track. For doing this interpolation, the orbit error was assumed to be a second-degree polynomial. Finally, a cosine lowpass filter with a cutoff wavelength of 150 km was applied to the data. Deviations from the average were then calculated along each track.

3. Results

As shown in Fig. 2, two 3-day coverages separated by roughly half a period of the expected wavelike signal exhibit opposite phases. This can be considered as an indication that the results are physical. In agreement with the results of Cheney et al. (1983), they reveal that the topography signal is less visible south of the equator

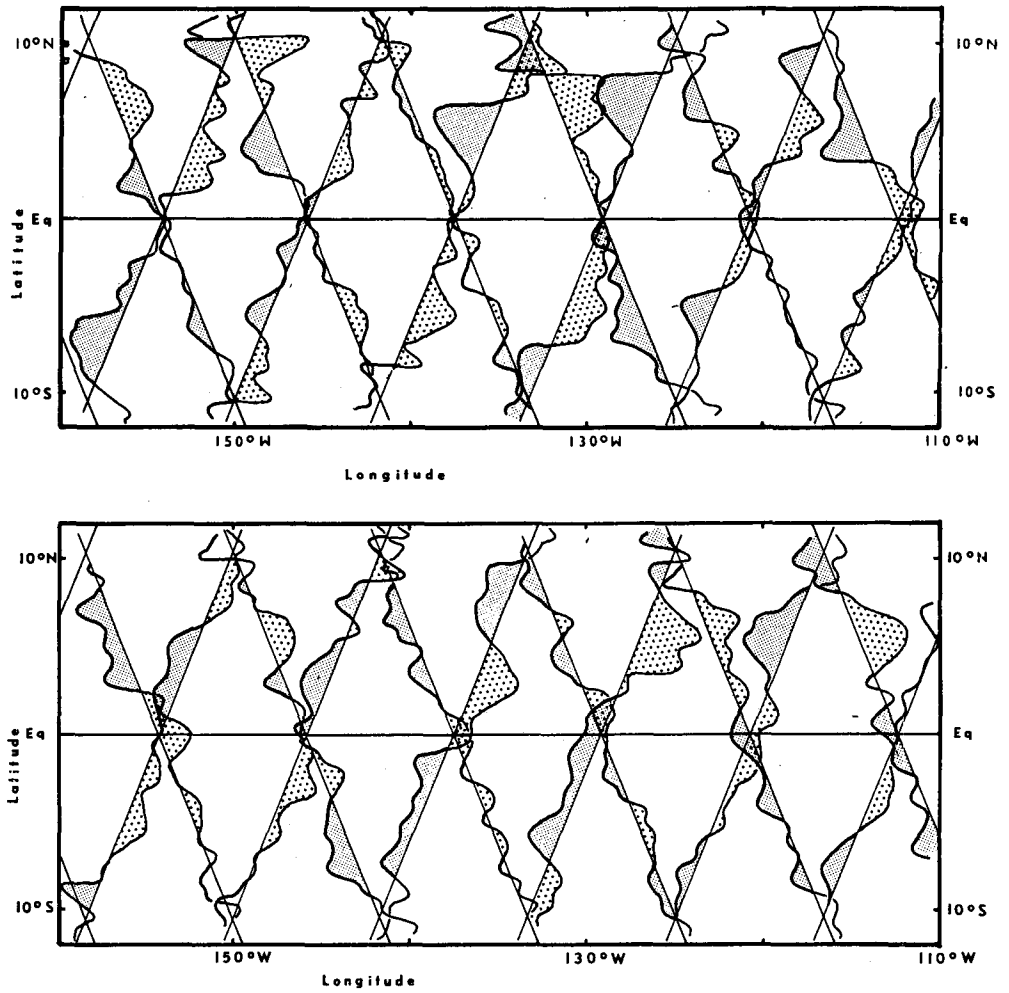

FIG. 2. Three-day projections of the Seasat dynamics topography relative to the 24-day average along the satellite tracks for (a) the first and (b) the sixth coverage, separated in time by roughly a half-period (15 days).

than north of it. Also, maxima of the order of 10 cm are observed near 4.5°N, alternating with minima of the same order. Finally, it was found that west of 160°W a significant signal also appears south of the equator.

The authors are well aware that noise is introduced in the signal at these latitudes, due to the very large water vapor content of the troposphere. Indeed, integrated water vapor contents of the order of 4.5 g cm^{-2} were estimated in these areas by the Seasat radiometer data (SMMR) algorithms (Chelton et al., 1981). This introduces a correction to the altimetric signal equivalent to 30 cm with a residual noise of about 3 cm rms (Tapley et al., 1982). In an analysis of Seasat altimetry data in the same area, Musman (1986) states that no significant difference is introduced by the use of FNOC rather than SMMR water vapor correction. L. Miller (personal communication) found that the difference between FNOC and SMMR corrections could be described by structures similar to the ones we are analyzing, but with much smaller amplitudes.

An objective analysis scheme (OA; described in De Mey, 1983; De Mey and Robinson, 1987; De Mey and Ménard, 1987) is used to map the variable signal. The OA was a space–time scheme, in that it made use of future and past data to calculate an estimate at an interpolation point. A phase speed was built in the OA to propagate information along selected characteristics. The maps are presented in Fig. 3. The center dates for the interpolation are the center dates for each 3-day coverage of the satellite on its repetitive orbit. A decorrelation length of 500 km (a half-wavelength), a temporal *e*-folding of 25 days along the characteristics, and a westward phase velocity of 40 km day^{-1} were selected in the analysis.

North of the equator, these maps clearly evidence the presence of alternate positive and negative signals. The trough-to-crest amplitude of the signal ranges from about 11 cm in the east to 15 cm in the west. The OA expected error in amplitude is of the order of 15% of the restored signal, assuming a 5 cm white noise in the data. This noise level only corresponds to the instrument noise. Additional noise is due to the various corrections applied to the measurements. These residual correction errors are dominated by the sea state bias, which should not be a major difficulty in our area, since the significant wave height is less than 2 m on the average (Chelton et al., 1981). The residual error, of the order of 0.6% of $H_{1/3}$ (Douglas and Agreen, 1983) is thus less than 2 cm. Also, this 5 cm error is consistent with the variability signal south of the equator, which includes the measurement noise and the correction residual errors.

The maps are consistent with previous knowledge concerning the westward displacement of the features. Since the restored velocity (40 km day^{-1}) is precisely the same as was specified in the OA, this result might be suspected to be a mere artifact of the analysis scheme. The sensitivity was tested for different OA parameter values (i.e., different decorrelation lengths, *e*-folding times, and propagation velocities). In particular, a version of the OA with zero built-in propagation was run on the Seasat residuals. Although the shape of the eddies was different, their propagation was restored. The shape of the eddies is more poorly defined in the OA with zero propagation, west of the 165°W. This could indicate that the nonzero built-in propagation in Fig. 3 artificially carries the features beyond the seamount range near 165°W.

South of the equator, the signal is much less intense and rarely exceeds 5 cm. This is probably within the altimeter noise, except for the strongest features, which appear generally aligned with their counterpart north of the equator. West of 165°W, the wave pattern is no longer visible, and the field exhibits turbulentlike characteristics. It is believed that bottom topography effects here play an important role in geographically separating both regimes.

Figure 4 presents maps of "absolute" dynamic topography north of the equator. With respect to Fig. 3, a stationary ridge model topography has been added. It models the ridge in the surface dynamic height field between the South Equatorial Current (SEC) and North Equatorial Counter Current (NECC). This model is similar to the kinematic model proposed by Miller et al. (1985). It was adjusted so that the troughs in the wave pattern be zeroed. Segments of the thermal front as inferred by Legeckis (1982) are represented on the maps. Their position correlates very well with the first open streamline south of the features. This is in agreement with Miller et al. (1985) and is another indication that the oscillations of surface topography and the SST waves have a link of causality between them or with a third process.

4. Discussion

It is possible to derive a number of parameters concerning the eddy field from the Seasat residuals. For example, their typical "significant" diameter is of the order of 600 km. This corresponds to the diameter of excess topography above the SEC/NECC ridge. It is much larger than the typical 140 km scale of eddies near 10°N; this is not surprising, as the present eddies are positioned close to the area of distinctive equatorial dynamics (see Siedler, 1983).

Assuming that geostrophy is still valid on the northern flank of the eddies, it can be estimated that the typical instantaneous velocity of a water particle on this flank is 0.7 m s^{-1}. This is close to the surface drifters velocities (Hansen and Paul, 1984). It is also slightly larger than the westward phase velocity of the eddies, which might indicate that some degree of nonlinearity is present in the wave system and that some water is transported along.

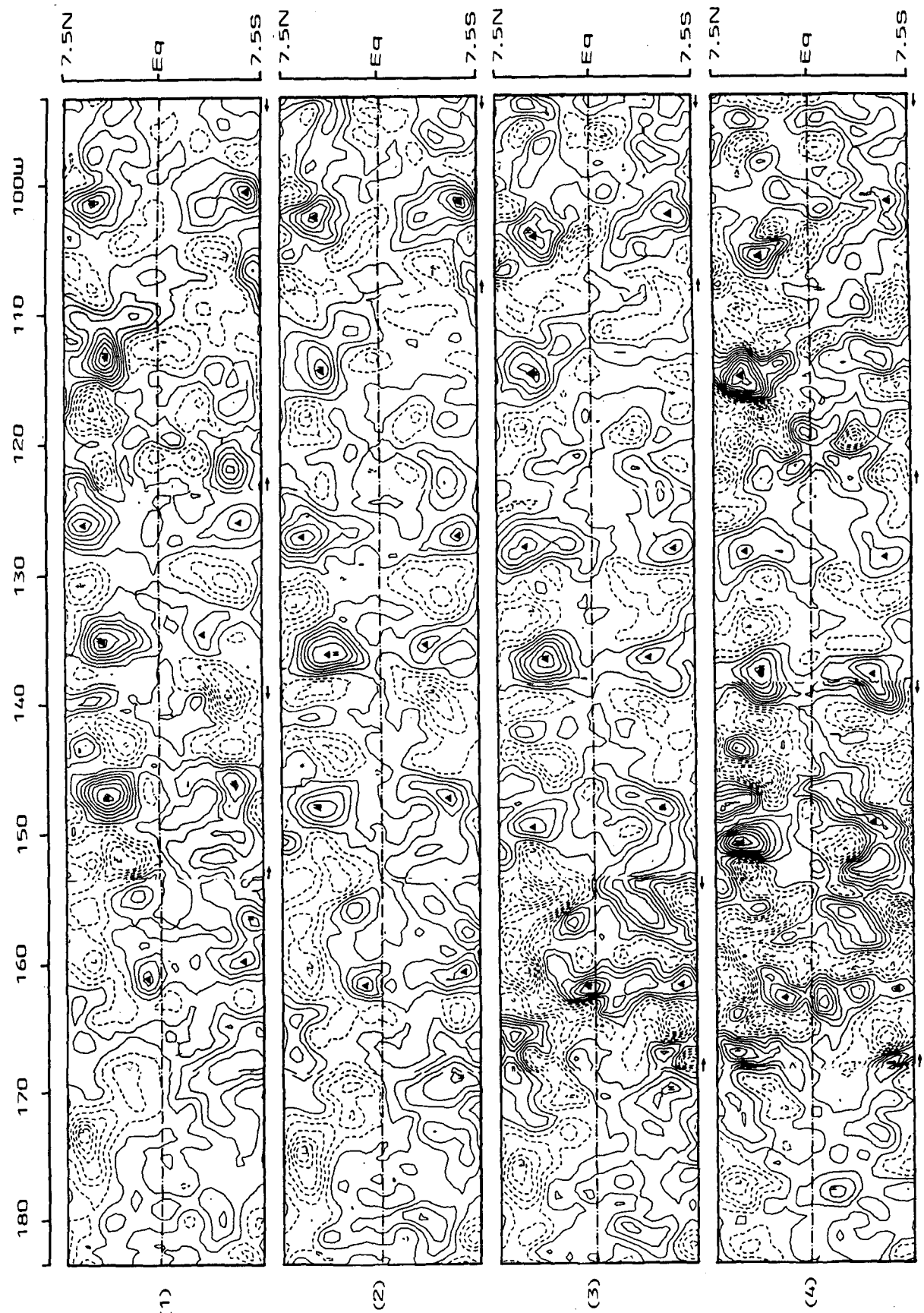

FIG. 3. Dynamic topography mapped by an objective analysis scheme. The times of the maps are the center times of each three-day Seasat coverage on its repetitive orbit. The triangle marks indicate the main persistent features with a positive topography signature. Contour interval: 2 cm, except for areas between arrows for which the contour interval is 1 cm.

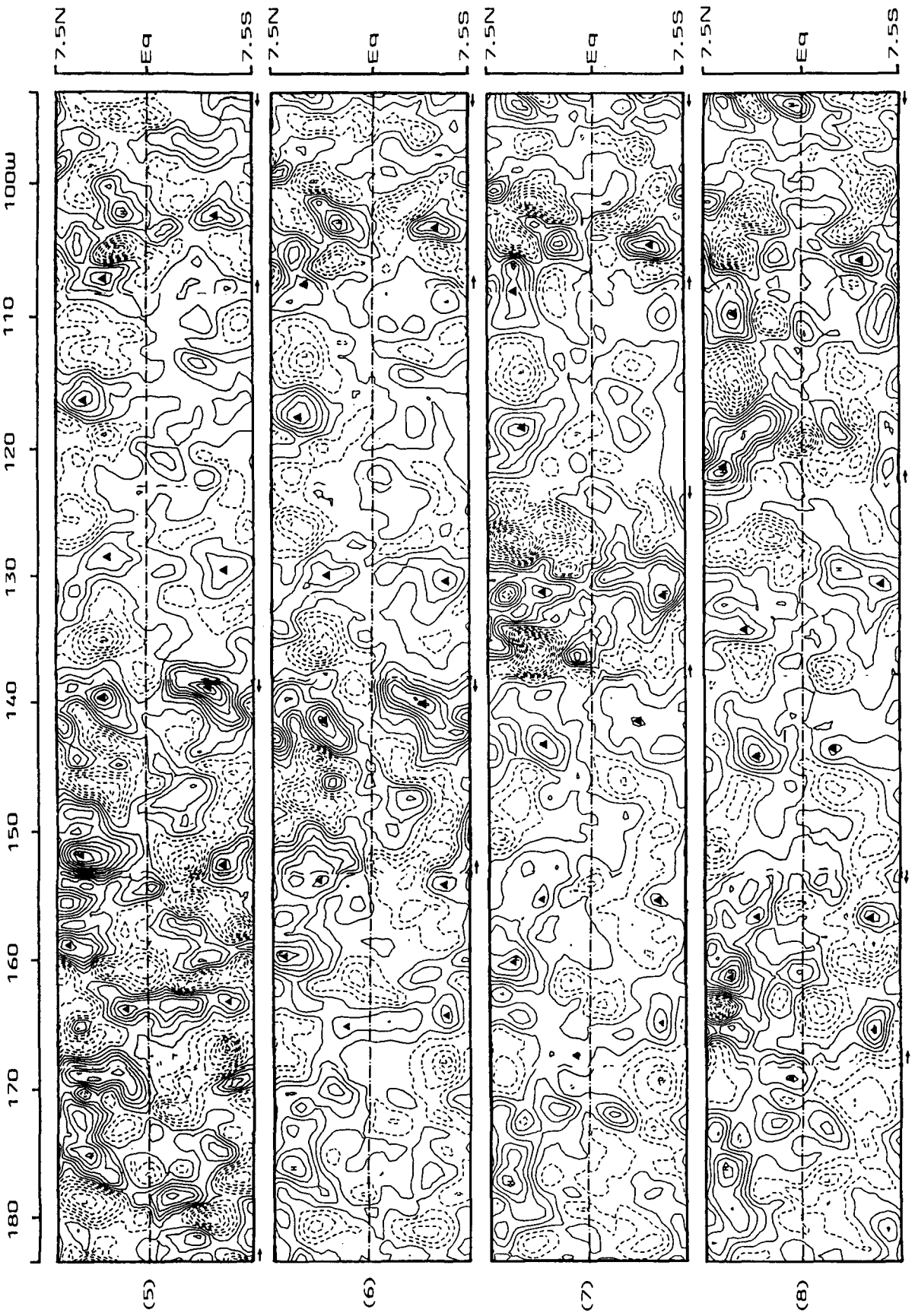

FIG. 3. (*Continued*)

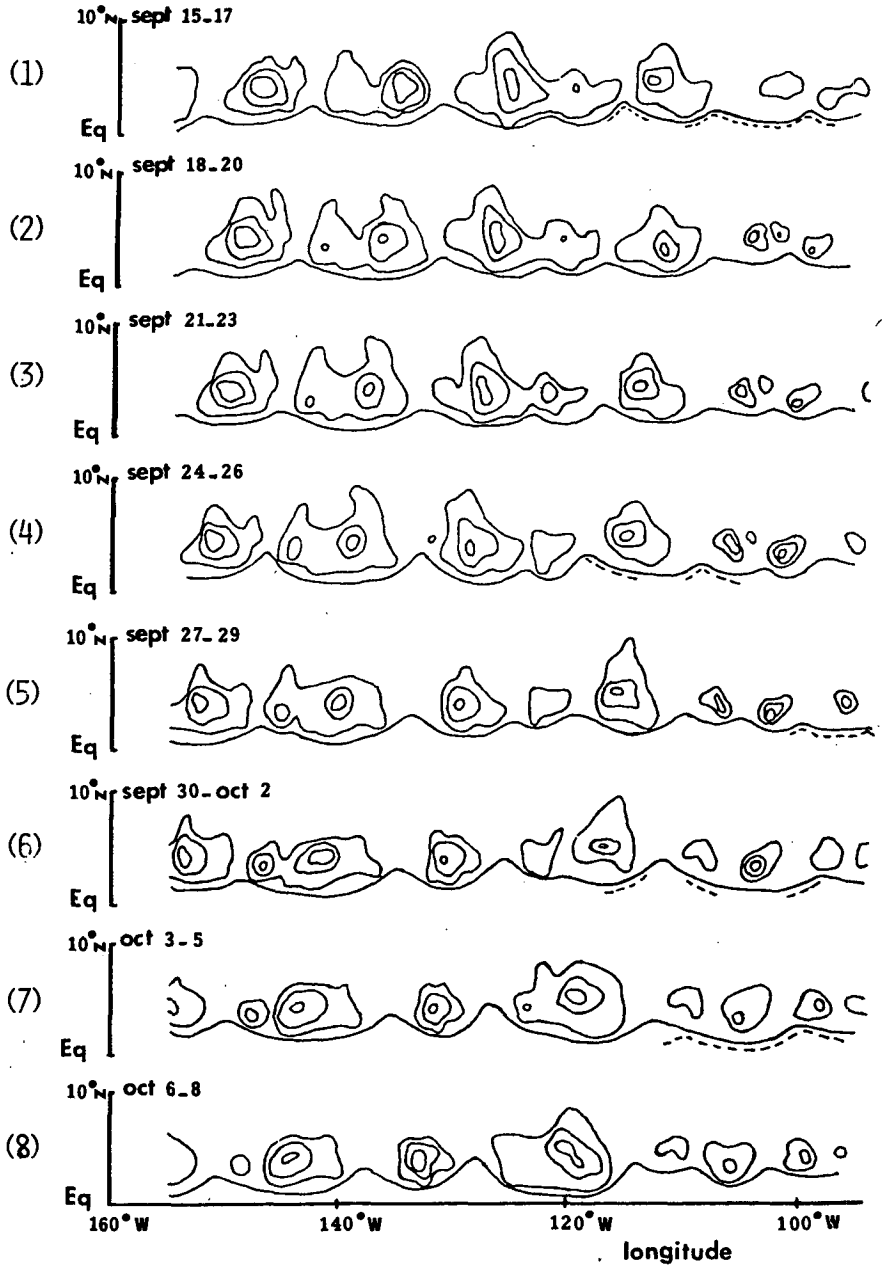

FIG. 4. As in Fig. 3 with the addition of a stationary ridge model topography. The dotted lines are for segments of the thermal front observed from surface temperature data (Legeckis, 1982). Contour interval: 5 cm.

Both sea surface temperature maps (Bernstein, 1984) and sea-level measurements (Philander et al., 1985; Miller et al., 1985) hint at the presence of a system of waves with wavelengths increasing northward. Indeed, some complexity seems to appear in the dynamic topography. First, the signal is more intense in the west than in the east. Second, there seems to be a superposition of "fast" and "slow" features (Fig. 4), which may interact with each other. Third, we have shown that some nonlinearity might be present in the system. Whether this corresponds to something real remains to be ascertained. The space–time sampling of Seasat on its repetitive orbit, and the accuracy of the data are only marginally sufficient for drawing dynamical conclusions about these waves. Better performance can be expected from future missions such as ERS-1 and TOPEX/POSEIDON.

Acknowledgments. This work benefited from fruitful discussions with Jean-Yves Gautier, Gilles Reverdin

(LODYC), Laury Miller (NOAA/NGS), Randy Watts and Mark Wimbush (University of Rhode Island), and Jacques Merle (LODYC). The altimeter data were preselected by Claude Brossier (CNES/GRGS).

REFERENCES

Bernstein, R. L., 1984: Satellite sea surface temperature determination from microwave and infrared radiometry. *Large-Scale Oceanographic Experiments and Satellites,* C. Gautier and M. Fieux, Eds., NATO ASI Series, Vol. 128, 87–98.

Chelton, D. B., K. J. Hussey and M. E. Parke, 1981: Global satellite measurements of water vapor, wind speed and wave height. *Nature,* **294,** 529–532.

Cheney, R. E., J. G. Marsh and B. D. Beckley, 1983: Global mesoscale variability from colinear tracks of Seasat altimeter data. *J. Geophys. Res.,* **88,** 4343–4354.

Colton, M. T., and R. R. P. Chase, 1983: Interaction of the Antarctic Circumpolar Current with bottom topography: An investigation using satellite altimetry. *J. Geophys. Res.,* **88,** 1825–1843.

Cox, M. D., 1980: Generation and propagation of 30-day waves in a numerical model of the Pacific. *J. Phys. Oceanogr.,* **10,** 681–686.

De Mey, P., 1983: Contribution à l'étude d'un tourbillon isolé: l'expérience Tourbillon-79. Docteur-Ingénieur Thesis, Ecole Nationale des Ponts et Chaussées, Paris, 144 pp.

——, and Y. Ménard, 1987: Analysis and assimilation of altimeter residuals and in situ measurements in the Polymode area. *J. Geophys. Res.* (in press).

——, and A. R. Robinson, 1987: Simulation and assimilation of satellite altimeter data on the oceanic mesoscale. *J. Phys. Oceanogr.* (in press.)

Douglas, B. C., and R. E. Agreen, 1983: The sea-state correction for Geos-3 and Seasat satellite altimeter data. *J. Geophys. Res.,* **88,** 1635–1661.

Hansen, D. V., and C. A. Paul, 1984: Genesis and effects of long waves in the equatorial Pacific. *J. Geophys. Res.,* **89,** 10431–10440.

Legeckis, R., 1977: Long waves in the eastern equatorial ocean: a view from a geostationary satellite. *Science,* **197,** 1167–1181.

——, 1982: Satellite infrared observations of oceanic long waves in the eastern equatorial Pacific from 1975 to 1981. NOAA Tech. Report NESS 92, 1–22.

——, W. Pichel and G. Nesierczuk, 1983: Equatorial long waves in geostationary satellite observations and in a multichannel sea surface temperature analysis. *Bull. Amer. Meteor. Soc.,* **64,** 133–139.

Miller, L., D. R. Watts and M. Wimbush, 1985: Oscillations of dynamic topography in the eastern equatorial Pacific. *J. Phys. Oceanogr.,* **15,** 1759–1770.

Musman, S., 1986: Sea slope associated with westward-propagating equatorial temperature fluctuations. *J. Geophys. Res.,* **91,** 10753–10757.

Périgaud, C., J.-F. Minster and G. Reverdin, 1986: Zonal slope variability of the tropical Indian Ocean studied from Seasat altimetry. *Mar. Geod.,* **10,** 53–68.

Philander, S. G. H., 1978: Instabilities of zonal equatorial currents: II. *J. Geophys. Res.,* **83,** 3679–3682.

——, D. Halpern, D. Hansen, R. Legeckis, M. Laury, C. Paul, D. R. Watts, R. Weisberg and M. Wimbush, 1985: Long waves in the equatorial Pacific Ocean. *Trans. Amer. Geophys. Union,* **66,** 154.

Schwiderski, E. W., 1980: On charting global ocean tides. *Rev. Geophys. Space Phys.,* **18,** 243–268.

Siedler, G., 1983: Tropical and equatorial regions. *Eddies in Marine Science,* A. R. Robinson, Ed., Springer-Verlag, 181–199.

Tapley, B. D., G. H. Born and M. E. Parke, 1982: The Seasat altimeter data and its accuracy assessment. *J. Geophys. Res.,* **87,** 3179–3188.

Weissberg, R. H., and A. M. Horigan, 1981: Low-frequency variability in the equatorial Atlantic. *J. Phys. Oceanogr.,* **11,** 913–920.

——, A. M. Horigan and C. Colin, 1979: Equatorially trapped Rossby-gravity wave propagation in the Gulf of Guinea. *J. Mar. Res.,* **37,** 67–86.

Wyrtki, K., 1978: Lateral oscillations of the Pacific equatorial countercurrent. *J. Phys. Oceanogr.,* **8,** 530–532.